Increasing Nano-Particle Dispersion Ratio in the Bubble Stretching-Based Technique

Fei Wang, Xiaoming Wang, Fang Chen, Xuezeng Zhao

School of Mechanical and Electronic Engineering, Harbin Institute of Technology, Harbin 150001, China

ABSTRACT: We present a new method to increase nano-particle migration rate in bubble stretching-based technique. Vibration created by the inflation and shrinking process of bubbles is used. Process parameters can be adjusted to increase the probability of collision between the nano-particles and the bubble wall. In effect, particles sufficiently migrate to the bubble wall, increasing both particle migration rate and dispersion ratio. Our measurement show that: (1) particle diameter, initial bubble radius, and initial bubble pressure strongly influence the migration of particles; (2) with appropriate parameters, nano-particles can quickly and efficiently migrate to the bubble wall through this new method. © 2011 Wiley Periodicals, Inc. J Appl Polym Sci 124: 3940–3946, 2012

Key words: particle dispersion; migration rate; bubble stretching; bubble vibration

INTRODUCTION

Nano-composites, such as nano TiO_2/polypropylene, polyethylene/montmorillonoid, etc., are widely used because of their satisfactory physical and functional properties. However, the high surface activity of nano-particles causes them to easily bond with other atoms, leading to agglomeration. The large nano-particle aggregates formed have sizes that are usually far beyond the nano-scale. Hence, they lose their nano-size effect, such as macroscopic quantum tunneling effect, etc. [1–4] Preventing the agglomeration of nano-particles during the process of preparing nano-composites, so that nano-particles can be dispersed evenly into polymers substrates, are key issues that directly affect the quality and efficiency of nano-composites.[5–8] Consequently, the bubble sketching-based nano-particle dispersion technique is used because it is less limited by material dispersion.[6–8] In this method, the high-speed stretch created by the inflation and blast of bubbles can effectively prevent aggregates and disperse nano-particles adsorbed on the bubble wall. However, experiments have shown that the practical dispersion ratio of this method is much lower than expected because the migration rate of particles onto the bubble wall is low, seriously affecting the dispersion of nano-particles. Therefore, increasing the migration ratio of nano-particles onto the bubble wall becomes a bottleneck problem in improving the applicability of the bubble sketching-based nano-particle dispersion method. This article reports a new method to increase particle migration rate in the bubble sketching-based nano-particle dispersion technique without changing the existing equipment. In this method, we use the vibration phenomenon created by the inflation process of bubbles. Process parameters, such as vibration frequency and the difference between internal and external pressure, can be adjusted to increase the probability of collision between nano-particles and the bubble wall. In effect, particles can sufficiently migrate to the bubble wall, significantly increasing the particle migration rate.

THEORY

During bubble formation in the bubble sketching-based technique, the bubble experiences a vibration process with its diameter alternately inflating and shrinking as long as the vibration energy is consumed. Afterward, the bubble vibration stops, and changes in the bubble radius become stable. We found that this vibration can be used to increase the migration rate of nano-particles.

In the bubble stretching-based nano-particle dispersion method, nano-particles within the bubbles have slower movement due to circulation within bubbles during their inflating process. Taking a
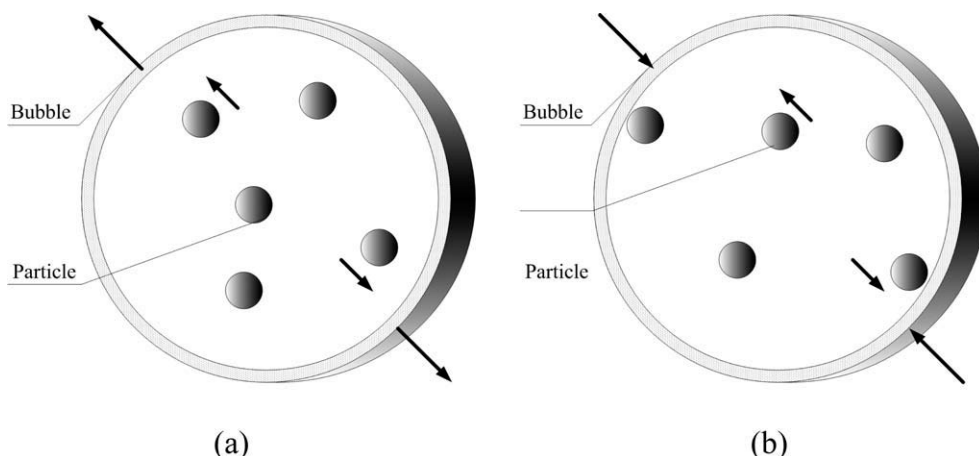
Figure 1 Schematic diagram of particle migration in bubbles: (a) during decelerated bubble inflation; (b) during accelerated bubble contraction.

single nano-particle for example [Fig. 1(a)], when the bubble inflates, the bubble airflow causes the nano-particle have slower migration than the bubble in the same direction of the inflating bubble. As the bubble radius increases, acceleration of the bubble inflation gradually decreases to zero. Furthermore, due to inertia, the bubble continuously inflates, while the inflation rate is gradually reduced. At this point, nano-particle movement is still accelerated. If the bubble vibration frequency and other parameters are appropriate, particles partially accelerate within the bubble, colliding with the bubble wall, which has a slower rate of movement. The particles then become attached to the bubble wall. In this article, the number of cycles that a bubble inflates and contracts in unit time is defined as the bubble vibration frequency. When the bubble vibration rate decreases to zero, the bubble begins to shrink. The airflow inside the air bubbles produces resistance against nano-particle movement toward the bubble wall [Fig. 1(b)]. Because of the inertia of the nano-particles, these continue to move toward the bubble wall while slowing down until their kinetic energy is completely consumed. The nano-particles accelerate in the same direction as bubble contraction. During bubble contraction and the deceleration of nano-particles, given proper parameters (e.g., bubble vibration frequency), both the bubble wall and nano-particles have enough time to move in opposite directions. In effect, a large number of nano-particles collide and adhere to the bubble wall, increasing the migration ratio of particles. All these movements occur repeatedly.

SIMULATION

To quantitatively analyze the particles in their migration process within the vibrating bubbles,

models for bubble vibration and particle motion were first established. The control equation of bubble vibration [eq. (1)] can be obtained using the continuity equation, the equation of motion, the equilibrium equation of bubble wall, the constitutive equation, Fick's Law, Henry's Law, and the ideal gas law.[9–11]

$$
\rho\left(\ddot{R}R + \frac{3}{2}\dot{R}^2\right) = P_g - P_b - \frac{2\sigma}{R}
$$
$$
- \frac{12\eta_0}{\lambda}\int_0^t e^{(s-t)/\lambda}\frac{R^2(s)\dot{R}(s)}{R^3(t)-R^3(s)}\ln\left(\frac{R(t)}{R(s)}\right)ds \quad (1)
$$

where R and P_g are the diameter and pressure of the bubble, respectively; P_b and ρ are the pressure and density of the polymer melt, respectively; σ is the surface tension between the gas and fluid; and η_0 and λ are the viscosity and relaxation time of the polymer melt, respectively.

Equation (1) can be further transformed to obtain the following equation:

$$
\ddot{R} = \frac{P_{g0}}{R\rho} - \frac{2\sigma}{\rho R^2} - \frac{P_b}{R\rho}
$$
$$
- \frac{12\eta_0}{\lambda R\rho}\int_0^t e^{(s-t)/\lambda}\frac{R^2(s)\dot{R}(s)}{R^3(t)-R^3(s)}\ln\left(\frac{R(t)}{R(s)}\right)ds - \frac{3\dot{R}}{2R\rho}
$$
$$
(2)
$$

From eq. (2), we can conclude that initial pressure, initial radius of the bubble, and polymer melt viscosity strongly influence the vibration of bubbles. Specifically, the initial pressure inside bubbles provides enormous implications on the vibration of bubbles with increased vibration amplitudes and initial bubble pressure. The bubble radius quickly reaches its maximum during the initial period, while bubble

frequency decreases as the initial pressure increases. Similarly, the greater the initial bubble radius, the greater is the vibration amplitude of bubble inflation and the smaller the bubble vibration frequency. In addition, the polymer melt viscosity provides a deterrent to bubble inflation. Hence, the smaller the viscosity, the greater is the bubble vibration amplitude. The smaller the viscosity, the smaller is the bubble vibration frequency.

During the bubble vibration process, nano-particles suspended within air bubbles are driven by the airflow inside air bubbles (and, around the same time, by the Brownian motion as well) to lag behind the bubbles because of the imbalance from particle collision. In such a motion process, particles are affected by gravity and lift. When selecting an individual particle to be studied, its equation of motion can be obtained according to Newton's second law of motion.

$$dv_p/dt = 18\mu_g(v_g - v_p)/\rho_p d_p^2 c_c + g + B(t) \qquad (3)$$

where v_p, d_p, and ρ_p represent the phase velocity vector, diameter, and density of the particles, respectively; v_g and μ_g represent the velocity vector and kinetic viscosity of gases, respectively; and c_c is the drag force correction factor in air for the submicron particles.[12] $B(t)$ is the Brownian motion diffusion force of particles whose components are:

$$B_i = Z_i\sqrt{2\pi s_0/\Delta t}, \; s_0 = 216\mu_g kT/\pi^2 d_p^5 \rho_p^2 c_c \qquad (4)$$

where Z_i is a random number of normal distribution with a mean of 0 and a variance of 1; k is the Boltzmann constant; and Δt is the time step. To accurately describe the Brownian particle movement rule, a Δt that is much longer than the time scale of gas molecules but shorter than the time of relaxation for particles must be selected.

Only the viscous drag and Brownian motion diffusion force are considered with respect to the particle motion equation. The particle has a smaller diameter, and it does not stay near the wall with a large velocity gradient. Hence, the effects of gravity and Saffman lift force are ignored.

From eq. (3), we can find that particle diameter and gas kinetic viscosity strongly influence particle motion.[12] Specifically, for particles of the same material, their different diameters provide different related inertia, and airflow within air bubbles play different roles. Therefore, the smaller the particle diameter, the smaller the particle inertia, and the greater is the impact of the airflow within the air bubbles as well as the amplitude of periodic motion. In contrast, a larger particle diameter leads to a larger inertia, smaller impact of the subject to the

vibration of air bubbles, and smaller amplitude of motion. Under a different gas kinetic viscosity, circulation affects the particles inside the bubbles differently. A greater gas kinetic viscosity results in a greater impact of the airflow on particle vibration that leads it to lag behind the bubble. It also leads to a smaller change in the trajectory influenced by the Brownian motion and to a smaller discrepancy among the particle trajectory, bubble inflation, and vibration trajectory. In contrast, a smaller gas kinetic viscosity results in a smaller impact of the airflow on particle vibration that leads it to lag behind the bubble, a larger change in the trajectory influenced by the Brownian motion, and a greater inconsistency of the particle trajectory with the bubble inflation and vibration trajectory.

Based on the bubble vibration and particle motion equations presented above, we have simulated particle migration within vibrating bubbles and calculated the migration ratio under different parameters. Combinations of the parameters have been found to increase the particle migration ratio. In the simulation, we assumed that particles passing through the air bubble wall are adsorbed by polymers. Particles can be considered to migrate toward the bubble wall and then move along with the bubbles when the particle coordinates satisfy the following mathematical relationship:[13]

$$\sqrt{C_x^2 + C_y^2 + C_z^2} \geq R \qquad (5)$$

where C is the coordinate position of a particle, and R is the bubble radius.

In this article, the simulation is conducted at 20°C and standard atmospheric pressure in the process where air bubbles are used to disperse silicon dioxide particles in epoxy. In the simulation, we selected 1000 particles and assumed that they do not interact during their migration and that their initial location is a random distribution. We set the simulation step as 0.1 μs and simulation time as 1 s. At each time step, eq. (3) was used to determine the corresponding position of each particle, we applied a four-order Runge-Kutta method to solve the related numerical solution for the motion of all particles. This determined whether particles migrated to the bubble wall according to eq. (5).

Previous analysis has shown that once the polymer melts, particles, gases, and environmental parameters are determined. The three factors left are: initial bubble pressure, initial radius, and particle diameter. They strongly influence bubble vibration parameters and particle motion. To study the effect of the different parameters on particle migration, we changed the initial bubble pressure, initial bubble radius, and particle diameter to calculate the migration rate of

TABLE I
Migration Rate of Particles Under Different Initial Bubble Radii

Particle diameter (μm)	Initial bubble radius (μm)			
	50	100	150	250
0.5	0	0	0	0
1	7.3%	0	0	0
5	36.7%	25.6%	24.4%	0
10	36.2%	22.4%	19%	0

particles under different parameters. Simulation results show that a smaller initial bubble radius with a greater initial bubble pressure, easier migration of the particles within air bubbles toward the bubble wall, and a higher particle migration rate. Table I summarizes the migration rate of particles within the vibrating bubbles when the initial bubble pressure is 1 MPa and both the initial bubble radius and the particle diameter are changed. For particles of the same diameter, migration rate decreases as the bubble radius increases. For the same initial bubble radius, the migration rate of particles increases along with increasing particle diameter and, on reaching the maximum of 5 μm, decreases as the diameter increases (Table I). Under certain initial bubble pressure values, the particle migration rate reaches its maximum at 36.7% when the particle diameter is 5 μm and the initial bubble radius is 50 μm. Table II summarizes the migration rate of particles within vibrating bubbles when the initial bubble diameter is 50 μm and both the initial bubble pressure and the particle diameter have been changed. For particles of the same diameter, migration markedly increases as bubble pressure increases. For the same initial bubble pressure, the particle migration rate increases along with increasing particle diameter and, on reaching a maximum at 5 μm, decreases as the diameter increases (Table II). Under certain initial bubble radii, the particle migration rate reaches its maximum at 72.7% when the initial bubble pressure is 10 MPa and the initial bubble diameter is 50 μm. The analysis of the evolution of particle migration shown in Tables I and II can further verify the effects of different initial bubble pressures, initial bubble radii, and particle

diameters that influence the migration of particles within vibrating bubbles.

In analyzing various parameters that influence particle migration, various parameters are adjusted, so that the particle migration rate can be maximized within the inflating and vibrating bubbles. By analyzing and comparing the data, the best combination of parameters was found to involve an initial bubble radius of 5 mm, an initial bubble pressure of 10 MPa, a particle diameter of 5 μm, and a migration rate that reaches its maximum at 72.7%.

EXPERIMENTS

Based on related theoretical analyses, an experimental study was conducted for the evolution of particle migration within vibrating bubbles. We have chosen epoxy resin E-20 as the polymer melt material because it is soluble in acetone to a certain concentration and because it forms a transparent melt. In this way, changes in bubbles and particles can be easily observed. In addition, to facilitate observation of particle migration to the bubble wall, particles should have a darker color. Hence, we chose nano-structured lead oxide as the migrating particle material. The experimental apparatus included an air pump, compression chamber, observation tube, static mixer, fluidized bed, throttle, gas tank, camera, etc. (Fig. 2).

Figure 3 shows an operational flow chart for the experiment of particle migration within the vibrating bubbles, which can be divided into five steps:

1. Preparation of epoxy resin solution
   Solid epoxy resin E-20 was crushed and dissolved in acetone in a certain percentage to obtain the epoxy resin solution whose surface tension was 0.0297 N m^{-1} and the kinetic viscosity was 200 Pa s in case of 20°C, which was placed into the observation tube. In the dissolution process, to shorten the dissolution time, stirring was applied using a mixer, a viscometer was used for real-time measurements of the epoxy resin solution and, meanwhile, the amount of solid epoxy resin E-20 and acetone solution was appropriately regulated to obtain

TABLE II
Migration Rate of Particles Under Different Initial Pressures

Particle diameter (μm)	Initial bubble pressure (MPa)			
	0.5	1	5	10
0.5	0	0	2.1%	11%
1	5.5%	8.3%	22.6%	57.8%
5	26%	36.7%	56.4%	72.7%
10	25.1%	36.2%	51.4%	70.5%
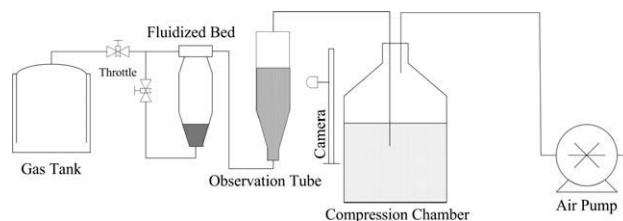
Figure 2 Schematic diagram of the experimental apparatus.
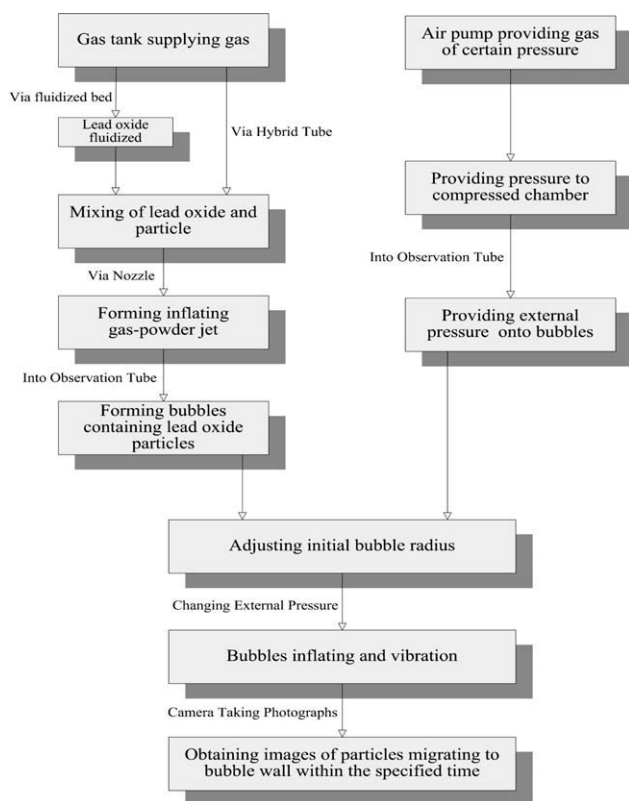
Figure 3 Experimental flow chart.

the solution whose parameters reached the requirements set. The prepared epoxy resin solution was a kind of light yellow transparent liquid in which bubbles can be more clearly observed to meet the experimental requirements. Then, the observation tube was filled with such prepared epoxy solution which was provided as the polymer melts, the external circumstance for the inflation and vibration of bubbles in the process of particle migration.

2. Formation of gas-powder-jet

The gas tank holds gas with a certain pressure, whose throttle should be adjusted to regulate the flowing velocity of gas and, under a certain flowing velocity, the gas flows into the fluidized bed. The lead oxide was fluidized in fluid-

ized bed under such an action. For particles of same density during the fluidization process, their inconsistent particle diameter would present significant regional differences while small particles would present small area of their activities and mostly concentrated at the top of the bed as particles could not reach the lower half. The activity area of large particles tended toward the lower, which was much greater than that of the small particles while the highly concentrated activity area of particles was at the lower half of the bed. Based on the fluidization of lead oxide particles, the throttle was adjusted to input gas under a certain velocity into the hybrid tube. When the compressed gas passed the hybrid tube in high velocity, there was a negative pressure zone formed in the hybrid tube, the lead oxide particles at the dilute phase zone in the fluidized bed would be sucked into the hybrid tube by the pressure action. Subsequently, lead oxide particles sucked into the hybrid tube would be fully mixed with gas driven by the high velocity of compressed gas. The mixed gas-powder was transferred to the nozzle at the bottom of the observation tube, by which the under-inflated gas-powder-jet was formed.

3. Formation of vibrating bubbles

The under-inflated gas-powder-jet was injected into the observation tube from its bottom to form small bubbles containing particles of lead oxide under some certain internal pressure. At this point, the viscosity of epoxy resin solution in the observation tube was 200 Pa s by which the bubbles into the observation tube would stay at a certain position of the observation tube. At the same time, the air pump was used to adjust the pressure of the observation tube so that the pressure of polymer solution in the observation tube could be similar to the gas pressure inside the bubbles and such bubbles would not be inflated at high speed while they were sprayed away from the nozzle.
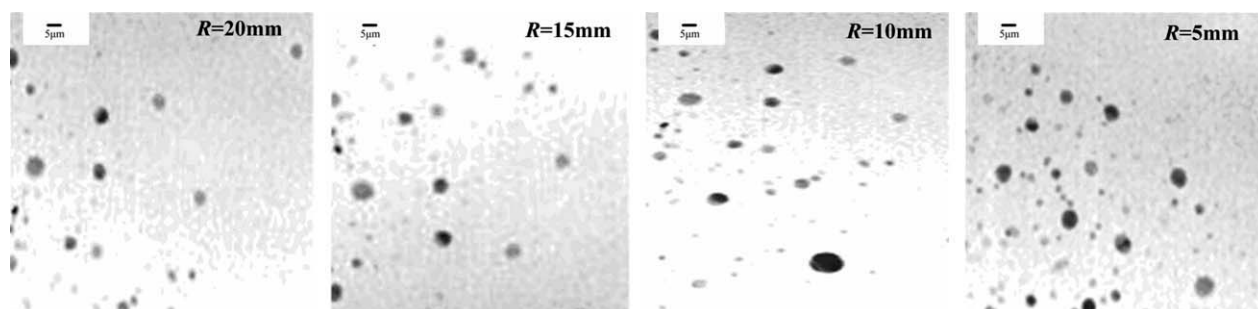
Figure 4 Tendency for migrating ratio of particles under different initial bubble radii.
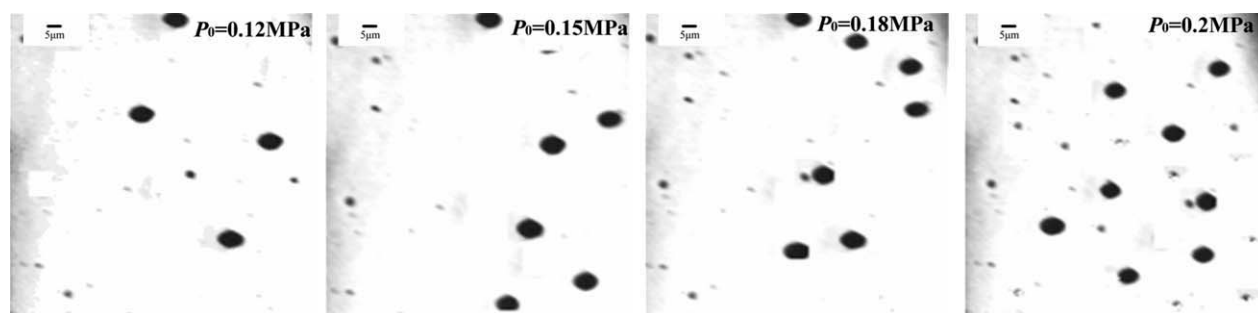
Figure 5 Tendency for migrating ratio of particles under different initial bubble pressures.

4. Adjustment of initial bubble radius

   When the bubbles entered and remained in the observation tube for a stable period of time, the gas pressure output by the pump was adjusted, the compression chamber was appropriately pressured to further indirectly provide slow pressure into the observation tube, i.e., increasing the external pressure onto bubbles. At this time, as the external pressure is greater than the internal pressure of bubbles, the bubbles would start to shrink because of the pressure difference of internal and external action. When the bubble radius was reduced to a pre-set value at which point the providing of pressure to the observation tube was stopped and the bubble radius was the initial radius of vibrating bubbles.

5. Observation of particle migration in vibrating bubbles

   When the initial radius of bubbles was compressed to the preset value, the pump output pressure was changed and the external pressure of bubbles was decreased so that the internal pressure could be greater than the external pressure and the bubbles would begin to inflate and vibrate under the pressure difference of internal and external action. Meanwhile, the particles within bubbles were driven by the airflow inside the bubbles to do their movement lagging behind the bubbles, and some particles would have collision with the bubble thus migrating onto the bubble wall. During the process of particle migration, the camera was used for taking photographs of the vibrating bubbles so as to obtain various images of particles migrating to the bubble wall within the specified time under different parameters. The obtained images were compared to further analyze the effects of various parameters impacting the particle migration within the vibrating bubbles.

According to the above steps, we conducted experiments on particle migration within the vibrating bubbles under different initial bubble radii and different initial bubble pressures. Figure 4 shows the migration tendency chart of particles migrating at 2 s at the bubble wall when the lead oxide particle diameter is 5 μm, the bubble pressure is 0.2 MPa, and the initial bubble radii are 20, 15, 10, and 5 mm. Figure 5 shows the migration tendency chart of particles migrating at 2 s at the bubble wall when the particle diameter is 5 μm, the initial bubble radius is 5 mm, and the bubble pressures are 0.12, 0.15, 0.18, and 0.2 MPa. The change in initial bubble pressure, initial bubble radius, during the process of bubble inflation and vibration can effectively increase the ratio of particles within the bubbles that migrate toward the bubble wall (Figs. 4 and 5). Furthermore, the experiments also show that the rate of particle migration inside the vibrating bubbles increases as the initial bubble pressure increases, and it decreases along with increasing initial bubble radius. All these are consistent with the evolution of particle migration obtained in the simulation using different parameters.

CONCLUSION

In summary, the migration of particles within vibrating bubbles has been studied in this article. Initially, the bubble vibration model and mathematical model of particle motion was introduced. The amplitude of bubble vibration depends on the initial bubble radius, initial bubble pressure, and polymer melt viscosity. Particle diameter and high gas kinetic viscosity affect on particle trajectories. Second, a mathematical model for classifying particle migration toward the bubble wall has been established. And the evolution of the migration rate of silicon dioxide particles in epoxy was analyzed under different parameters. Results showed that under certain melt viscosities, temperatures, and other conditions, particle migration rate decreases along with increasing bubble radius, while it increases along with increasing bubble pressure. Under certain initial bubble pressure and radius, the migration rate increases along with increasing particle diameter,

and the migration rate decreases along with increasing particle diameter when its maximum diameter reaches a certain value. In the comprehensive analysis of simulation data under different parameters, when the initial pressure is 10 MPa, the initial bubble radius is 50 μm, and the particle diameter is 5 μm, the migration rate reaches its maximum at 72.7%. The experimental results showed that the evolution of particle migration is consistent with the simulated results. This article has provided a simple method for increasing the scatter coefficient of the bubble inflation-based nano-particle dispersion technique. The technique used the vibration of bubbles to quickly and efficiently migrate particles within the bubbles to the bubble wall without changing the context of the existing equipment.

References

1. Yan, Y.; Tholen, A. R. Nanostruct Mater 1999, 12, 661.
2. Alymov, M. I.; Shorshorov M. Kh. Nanostruct Mater 1999, 12, 365.
3. Kawasumi, M. J Polym Sci Part A: Polym Chem 2004, 42, 819.
4. Sudduth, R. D. J Appl Polym Sci 1994, 52, 985.
5. Mackay, M. E.; Tuteja, A.; Duxbury, P. M.; Hawker, C. J.; Horn, B. V.; Guan, Z.; Chen, G. H.; Krishnan, R. S. Science 2006, 311, 1740.
6. Wu, D. M.; Meng, Q. Y.; Liu, Y.; Ding, Y. M.; Chen, W. H.; Xu, H.; Ren, D. Y. J Polym Sci Part B: Polym Phys 2003, 41, 1051.
7. Meng, Q. Y.; Wu, D. M. Phys Lett A 2004, 327, 61.
8. Zheng, X. T.; Wu, D. M.; Meng, Q. Y.; Wang, K. J.; Liu, Y.; Wan, L.; Ren, D. Y. J Polym Res 2008, 15, 59.
9. Yoo, H. J.; Han, C. D. AIChE J 1982, 28, 98.
10. Yoo, H. J.; Han, C. D. Polym Eng Sci 1981, 21, 69.
11. Han, C. D.; Yoo, H. J. Polym Eng Sci 1981, 21, 518.
12. Ounis, H.; Ahmandi, G.; McLaughlin, J. B. J Colloid Interface Sci 1991, 147, 233.
13. Laker, T. S.; Ghiaasiaan, S. M. J Aerosol Sci 2004, 35, 73.